NASA TECHNICAL NOTE

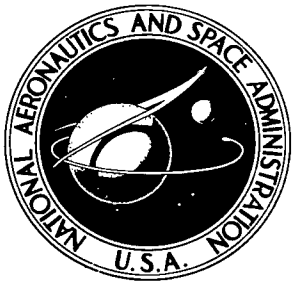

NASA TN D-7051

EFFECTS OF COLD WORK AND AGING ON THE SUBSTRUCTURE AND PRECIPITATION PHENOMENA IN THE COBALT-BASE ALLOY L-605

by Gary D. Sandrock and Charles W. Andrews

Lewis Research Center
Cleveland, Ohio 44135

NATIONAL AERONAUTICS AND SPACE ADMINISTRATION • WASHINGTON, D. C. • FEBRUARY 1971

1. Report No.	2. Government Accession No.	3. Recipient's Catalog No.
NASA TN D-7051		

4. Title and Subtitle: EFFECTS OF COLD WORK AND AGING ON THE SUBSTRUCTURE AND PRECIPITATION PHENOMENA IN THE COBALT-BASE ALLOY L-605

5. Report Date: February 1971

6. Performing Organization Code:

7. Author(s): Gary D. Sandrock and Charles W. Andrews

8. Performing Organization Report No.: E-5959

10. Work Unit No.: 129-03

9. Performing Organization Name and Address:
Lewis Research Center
National Aeronautics and Space Administration
Cleveland, Ohio 44135

11. Contract or Grant No.:

13. Type of Report and Period Covered: Technical Note

12. Sponsoring Agency Name and Address:
National Aeronautics and Space Administration
Washington, D.C. 20546

14. Sponsoring Agency Code:

15. Supplementary Notes:

16. Abstract

A thin-foil electron microscopy study was made of the cobalt-base alloy L-605 in four conditions: mill-annealed; mill-annealed and cold-worked; mill-annealed and aged; and mill-annealed, cold-worked, and aged. Cold-working produced bands of extended dislocations on two or more octahedral slip systems, one predominant; their density increased with degree of cold work. Aging collapsed nearly all extended dislocations. Cold-working prior to aging promoted intragranular nucleation, producing a more uniform distribution of precipitation. Severe cold-working plus aging produced evidence of partial recrystallization.

17. Key Words (Suggested by Author(s))	18. Distribution Statement
Cold working; Cobalt superalloy; Electron microscopy; Precipitation; Dislocations; Stacking faults; Ductility; Strength; Slip systems; Recrystallization; Grain boundaries	Unclassified - unlimited

19. Security Classif. (of this report)	20. Security Classif. (of this page)	21. No. of Pages	22. Price*
Unclassified	Unclassified	28	$3.00

*For sale by the National Technical Information Service, Springfield, Virginia 22151

EFFECTS OF COLD WORK AND AGING ON THE SUBSTRUCTURE AND PRECIPITATION PHENOMENA IN THE COBALT-BASE ALLOY L-605

by Gary D. Sandrock and Charles W. Andrews

Lewis Research Center

SUMMARY

A thin-foil electron microscopy study was made of the cobalt-base alloy L-605 (HS-25) in four conditions: mill-annealed; mill-annealed and cold-worked; mill-annealed and aged; and mill-annealed, cold-worked, and aged. Rolling reductions were 5 and 30 percent. The aging temperature was 1600° F (871° C), and aging time was 1 hour with two exceptions. One specimen was examined as cold-rolled 5 percent and aged 7 hours, and one was examined as cold-rolled 30 percent and aged 50 hours. The thin foils were prepared as disk specimens by mechanical and electrolytic thinning.

Cold-working produced bands of extended dislocations with numerous areas containing long stacking faults. Analysis of electron micrographs indicated that primary slip activity had occurred on one octahedral plane, with subsequent slip activity taking place on one or more secondary octahedral planes and causing shearing of the primary slipbands. The density and thickness of the slipbands increased with degree of cold work. Aging caused nearly all of the extended dislocations to collapse and stacking faults to disappear. Arrays and networks of total dislocations then appeared to delineate the former slipbands.

Cold-working prior to aging resulted in a more uniform distribution of precipitation nucleation sites, relative to aging directly from the annealed condition. Intersections of slipbands on two systems appeared to be especially favored sites. The present study verified the results of previous metallographic and mechanical properties observations of L-605 and extended the observations to the substructural level. These showed that prior cold-working reduced preferential grain boundary precipitation during aging and correspondingly increased the room-temperature ductility and the room-temperature tensile yield and ultimate strengths after aging. Without the cold work, embrittlement occurs in L-605 in some compositional ranges as a result of exposure in the 1600° F (871° C) temperature range and promotes premature intergranular tensile fracture at room temperature.

Substructural evidence of incipient or partial recrystallization was observed in samples which had been severely cold-rolled (30 percent) and aged (1 or 50 hr). This agrees with previous light microscopy and X-ray diffraction results for the same treatments.

INTRODUCTION

The application of transmission electron microscopy (TEM) to the study of superalloys (with emphasis on nickel-base alloys) was reviewed recently by Kotval (ref. 1). The major TEM work on cobalt-base superalloys has been performed by Lux and Bollmann at Battelle-Geneva and by a group at the Centre Nadional de Recherches Metallurgiques in Belgium (refs. 2 to 9). Recent work in this country has been done on the cobalt-base alloy Mar-M-509 (ref. 10). The cobalt-base alloy L-605 (HS-25) has also been studied by Yukawa and Sato in Japan (ref. 11). However, most of their work was concerned with material that was solution-annealed and aged without intervening cold work.

The purpose of this report is to characterize the substructures developed in L-605 (HS-25) by various cold-working and aging treatments. A further purpose is to relate these substructures to corresponding previously determined light-microscopy and mechanical-properties results for this alloy (ref. 12).

The alloy L-605 is subject to embrittlement in certain compositional ranges. It was chosen for this study because cold-working before aging can reduce substantially its susceptibility to intergranular brittleness at room temperature as a result of heating in the 1600° F (871° C) realm (refs. 12 to 14). This behavior was shown by a prior study by one of the present authors using mechanical-properties measurements and light-microscopy and X-ray diffraction techniques (refs. 12 and 13). Based on the light-microscopy observations of aged microstructures, especially those adjacent to room-temperature tensile fractures, the ductility and strength improvements were attributed mainly to a reduction in preferential intergranular precipitation. Cold-working generated a profusion of nucleation sites within the grains. We wished to confirm and extend to finer detail these light-microscopy and X-ray diffraction results by examining by TEM the substructures resulting from the improved distribution of nucleation sites introduced by cold work between the annealing and aging treatments. We also wished to relate these substructures with the reported mechanical properties.

The present study concentrated on the aged condition (1600° F, 871° C) and compared the nucleation characteristics in the mill-annealed-and-cold-worked material with those in the mill-annealed material without cold work. The aging temperature was the same as that used in the earlier study (refs. 12 and 13) as a result of Wlodek's observation (ref. 15) that the maximum rate of high-temperature embrittlement occurred at this temperature. The cold work was achieved by rolling to reductions of 5 and 30 percent. Aging time was generally 1 hour except for one specimen aged for 7 hours and one for 50 hours.

GENERAL BACKGROUND

The TTT diagram given by Yukawa and Sato (ref. 11) for solution treated L-605 is produced here as figure 1. It gives the precipitate phases that can form during subsequent aging treatments. Table I gives the crystal structures and lattice parameters of these phases.

The following review of the main light-microscopy and mechanical-properties findings of references 12 and 13 forms the specific background against which the results of the present study are to be discussed. Figures 2 and 3 show the changes in tensile elongation and strength resulting from increasing degrees of prior cold work (rolling) for aging times of 50 and 1000 hours. Corresponding properties are also shown for various degrees of cold work without aging. It is evident that aging 50 hours greatly decreases the room-temperature tensile ductility of L-605 for the annealed or moderately cold-worked conditions and increases the ductility for 30- and 40-percent cold reductions. These effects are intensified by increasing the aging time to 1000 hours. Cold-rolling increases both the yield and the ultimate tensile strength of the unaged alloy, but aging significantly reduces the yield and ultimate tensile strengths of the material rolled 30 and 40 percent relative to those of the unaged alloy.

Light-microscopy results from reference 12 summarizing the effects of prior cold work on microstructure of unaged and aged (1600° F, 871° C) L-605 are shown in figures 4 and 5, and the relation between microstructure and fracture characteristics is illustrated in figure 6. Figure 4 illustrates the development, with increasing degree of cold reduction, of predominantly single slip (fig. 4(b)), followed by multiple slip on two or more systems (fig. 4(c)). The annealed structure is shown in figure 4(a) for comparison. In the corresponding aged (50 hr) microstructures shown in figure 5, it is apparent that the proportion of precipitate within the grains, relative to that in grain boundaries, increases distinctly with even 5 percent prior cold work (compare fig. 5(b) with 5(a)). Also, the favored sites for precipitation within the grains apparently are along slipbands developed by the prior cold work (compare fig. 5(b) with 4(b)). In figure 5(c)(30 percent prior cold work), intragranular precipitation has become so general and relatively uniform that it obscures the grain boundaries. Certainly this condition would be expected to provide much improved distribution of plastic deformation between grain boundaries and grain interiors over that shown in figure 5(a), with no prior cold work.

The fracture micrographs of figure 6 verify the preceding observation. With no prior cold work in the 1000-hour aged alloy, fracture clearly occurred during a room-temperature tensile test along grain boundaries where heavy precipitation was present. With 30-percent cold reduction prior to aging, a corresponding fracture was definitely transgranular and appeared significiantly more ductile; moreover, the grain boundaries were not delineated by intergranular precipitates.

While not apparent in the micrographs referred to previously, the study of reference 12 showed both metallographic and X-ray diffraction evidence of partial recrystallization after aging for 1000 hours, for the samples which had received the larger amounts of prior cold work (15 percent and greater). Partial recrystallization was considered to be at least partly responsible for the decrease in room-temperature tensile yield and ultimate strengths after aging relative to strengths for the unaged condition, shown in figure 3, for prior cold reductions of 30 and 40 percent.

MATERIALS AND PROCEDURE

Material from the same heat as that used in the studies of references 12 and 13 was used for the current research. Consequently, the light-microscopy and X-ray diffraction observations, and the mechanical properties results of references 12 and 13 provide the relevant background against which to interpret the TEM observations reported here. The composition of the L-605 heat used is shown in table II, along with the standard specification limits for the alloy (ref. 16). This heat contained enough silicon (on the high side of normal commercial practice) to promote the formation of the embrittling cobalt-tungsten Laves phase Co_2W (refs. 15, 17, and 18).

The details of the cold-working and aging procedures are given in reference 12. Briefly, 0.048-inch-(1.2-mm-) thick sheet was obtained from a commercial vendor in the mill-annealed condition, that is, heated at 2250° F (1232° C) and rapidly-air-cooled. The sheet was cold-rolled up to 30 percent (at room temperature) in passes of approximately 5 percent and then aged in air at 1600° F (871° C). In order to observe the early stages of precipitation, the aging times used in the present study were short relative to those of reference 12. They were 1 hour, with the exception of one sample aged 7 hours and another aged 50 hours. The treatments were as follows:

Cold reduction, percent	Aging time, hr
0	0
	1
5	0
	1
	7
30	0
	1
	50

The stages of specimen preparation prior to electropolishing to thin foils were as follows: Disks approximately 1/8 inch (3.2 mm) in diameter were trepanned by electrical discharge machining through the entire thickness of the sheets. The disks were then hand ground from both sides to a thickness of approximately 0.014 inch (0.35 mm), using wet 320-grit silicon carbide paper. More stock was removed from one face than from the other, so that the centerplane of the final specimen would be very nearly halfway between the surface and the centerplane of the original sheet. The 0.014-inch (0.35-mm) disks were then hand ground to 0.004-inch (0.1-mm) thickness by removing equal amounts from each face using wet 600-grit silicon carbide paper.

The 0.004-inch (0.1-mm) disk specimens were electrochemically thinned to perforation (to provide electron-transparent regions adjacent to the perforation) in a twin-submerged-jet apparatus. The electrolyte was 10 percent sulfuric acid in ethanol maintained at 0° to 5° C. Cell potentials used ranged from 30 to 60 volts. The higher values were generally required by the aged specimens.

The finished foils were examined in a JEM-7A electron microscope at an operating potential of 100 kilovolts using a goniometer stage.

RESULTS AND DISCUSSION

The results of this study will be presented and discussed in two parts. The first will consider the effect of cold reduction on the microstructure of unaged L-605. The second part will consider precipitation due to aging in L-605 with and without prior cold work.

Substructure of Cold-Worked Specimens

0-Percent cold reduction. - The substructure of the mill-annealed (or starting) material is shown in figure 7. A moderate density of stacking faults (extended dislocations) is present on two or more {111} planes of the face-centered-cubic (fcc) matrix. This is common in cobalt-base alloys, which generally have low stacking-fault energy (refs. 4 to 11). Some stacking faults are long and almost continuous (fig. 7(a)), while others exist as relatively short segments (fig. 7(b)). The characteristic fringes of the stacking faults, and the irregularly curved partial dislocations bounding them at each end are more apparent at the higher magnification of figure 7(c). The annealed substructure illustrated here gives rise to the relatively featureless light microstructure shown in figure 4(a). Strength is low and ductility is high (figs. 2 and 3).

5-Percent cold reduction. - The substructure of a specimen cold-rolled 5 percent is shown in figure 8. It is apparent that the density of stacking faults is higher here than in figure 7. Slip has occurred nonhomogeneously, being concentrated in bands or "bundles of stacking faults." These deformation bands tend to lie predominantly parallel to one another on parallel slip planes, indicating major slip activity was on a single system. However, evidence of slip activity on two secondary systems is also present (fig. 8(a)). Between the heavily deformed bands, "single" stacking faults similar to those characterizing the mill-annealed material are also evident (fig. 8(b)). Some of the slipbands are becoming apparent in light microstructures (fig. 4(b)), and while ductility remains high, room-temperature tensile strengths have increased significantly (figs. 2 and 3).

30-Percent cold reduction. - Substructures of samples with a higher degree of cold reduction (30 percent) are shown in figures 9(a) to (c). Deformation bands are much thicker and more dense than in the 5-percent-reduced specimens, and again it is evident that slip on a single system predominated (figs. 9(a) and (b)). However, it is also apparent that a second slip system later became active and sheared and distorted the primary deformation bands (fig. 9(a)). These characteristics are apparent also in figure 4(c); here a high density of distorted slipbands has developed in all grains. More details of this sequence are evident at the higher magnification of figure 9(b), which encompasses only four or five of the primary deformation bands.

A portion of one of the primary deformation bands is shown at yet a higher magnification in figure 9(c). This appears to consist of irregular, but essentially parallel, faulted regions, thicker than those resulting from the 5-percent cold reduction, plus dislocation tangles.

The 30-percent cold reduction effected an increase of approximately 90 percent in room-temperature yield strength and 80 percent in ultimate strength, as shown in figure 3. Hirsch, Howie, Nicholson, Pashley, and Whelan (ref. 19) have pointed out that a fine structure similar to that in the primary slipband of figure 9(c) has been observed to result from a martensitic transformation that occurred during electrothinning of the foil, in its thinner portions. This phenomenon has been attributed to reduction in the strain energy for the transformation due to the decrease in specimen thickness. It is unlikely to have occurred here, since the secondary-system slip appears to have displaced and fragmented the "primary" bands, and this is improbable after electrothinning. However, it also seems plausible that the thick lines parallel to the primary slipband may be stacking-fault fringes (as suggested previously in this section), which are overlapping or have been reduced to one or two fringes per stacking fault by the thinness of the foil in the region of the micrograph. The irregular, nonparallel appearance of some of the lines, and other peculiar contrast effects associated with them in figure 9(c), may result from the presence of hexagonal-close-packed (hcp) phase formed by severe cold-working and bounded by stacking faults. Yukawa and Sato identified the hcp matrix

phase by both X-ray diffraction and electron diffraction, in the "martensitic feature" of the L-605 they studied, after cold reductions of 20 percent and greater (ref. 11). They observed the hcp matrix regions to be very effective in nucleating coherent carbides and beta-Co_3W at lower aging temperatures and attributed the major age-hardening of the cold-worked alloy in the lower range of aging temperature (below 1472° F, 800° C) to this effect. Sandrock and Leonard (refs. 12 and 13) also found the hcp matrix phase by X-ray diffraction in the same 30-percent-cold-worked material being discussed here.

A selected-area-diffraction pattern of the region shown in figure 9(b) is reproduced in figure 9(d). Analysis of this pattern provided the following information: The plane of the foil is approximately (110). The heavy deformation bands lie on the (111) plane parallel to the $[1\bar{1}0]$ direction in the plane of the micrograph. The subsequently formed (secondary) slipbands, seen "edge-on" in figure 9, lie on $(1\bar{1}1)$ planes parallel to the $[\bar{1}12]$ direction in the plane of the micrograph. Note in figure 9(d) the thin, nearly continuous streaks (reciprocal-lattice "rel-rod") between many diffraction spots. These are normal to the fine "edge-on" slipbands of figure 9(b)(after taking account of rotations and inversions, which occur in the electron microscope, between the corresponding micrograph and diffraction pattern). They could in fact result from the presence of very thin (a few atom layers thick) regions of faulted hcp structure within the "edge-on" deformation bands. The shorter streaks in figure 9(d), normal to the primary deformation bands of figure 9(b), similarly appear to correspond to the thicker faulted hcp regions in these bands.

Substructure of Aged Specimens

0-Percent prior cold reduction. - The precipitation in L-605 from the annealed condition (with no prior cold work) has been studied in detail by Yukawa and Sato (ref. 11). For this reason we shall not emphasize this treatment but only present sufficient data to allow a comparison with the substructures of the cold-worked and aged material.

Figure 10 shows several features seen in thin-foil micrographs of material aged 1 hour at 1600° F (871° C) with no cold work prior to the aging. Several substructural features are evident. As seen before by light microscopy, nucleation takes place predominantly on grain boundaries (fig. 10(a)) and on annealing-twin boundaries (fig. 10(b)), with relatively little nucleation evident within the grains.

Kotval noted the effectiveness of stacking faults in nucleating carbides in superalloys (ref. 20), and Yukawa and Sato found them effective in nucleating Co_3W as well as carbides in L-605 (ref. 11). However, stacking faults in the densities observed in this study in the annealed material did not appear to be effective to any degree at the aging temperature used. In fact, most evidence of stacking faults disappeared with aging; the

extended dislocations collapsed to total dislocations and formed subgrain boundaries (dislocation arrays or networks) or dislocation tangles, as in figure 10(c). A few particles were observed to nucleate in these regions (figs. 10(d) and (e)), but their number was insignificant relative to those nucleating at grain and twin boundaries in accord with the corresponding light micrograph (fig. 5(a)). This predominance of grain-boundary and twin-boundary precipitation leads to intergranular or twin-boundary fracture and low ductility after high-temperature exposure (refs. 12 and 15), as shown in the light micrograph (fig. 6(a)).

5-Percent prior cold reduction. - Figure 11 shows the substructure of material cold-reduced 5 percent and aged 1 hour at 1600° F (871° C). Again most, but not all, of the extended partial dislocations have collapsed to total dislocations. The deformation bands which were observed in the corresponding cold-reduced condition (fig. 8) are still evident. However, they appear in figures 11(a) and (b) not as "bundles" of stacking faults, but rather as tangles or arrays of total dislocations, or occasional stacking faults. There is evidence in the micrographs of figure 11 that deformation bands, and especially their intersections, are preferred sites for nucleation of precipitates. The latter effect is particularly apparent in figure 11(c). Greater detail of precipitation at the intersections of tangles with a stacking fault is shown in figure 11(d).

Figure 12 illustrates the effect of aging the 5-percent-cold-reduced material for the longer time of 7 hours. There is evidence here of increased intragranular precipitation relative to that in specimens aged 1 hour without prior cold work (e.g., fig. 10); however, grain-boundary precipitation still predominated, as shown in figure 12(a). Note precipitation along grain boundary A-A, plus precipitate particles B and C within the grain, in figure 12. This is in keeping with previous light-microscopy observations (fig. 5(b)). In general, the precipitate particles were quite opaque to the 100-kilovolt electron beam, so that in situ diffraction patterns of them were difficult to obtain.

Occasionally atypical regions were found in the 5-percent-cold-reduced and aged substructures which were substantially different in appearance from those which have been discussed. For example, figure 13 shows a region containing a high density of stacking faults in a sample aged 7 hours. However, in general, evidence of stacking faults disappeared upon aging at 1600° F (871° C). It is possible that the stacking faults of figure 13 actually did not survive the aging treatment, but rather are "artifacts" introduced subsequently by accidental plastic deformation of the thin-foil specimen during preparation or handling.

30-Percent prior cold reduction. - The substructure of specimens cold-worked 30 percent and aged at 1600° F (871° C) is shown in figure 14. Aging time was 1 hour for the specimens shown in figures 14(a) to (c) and 50 hours for that shown in figure 14(d). Precipitation within the grains is extensive compared to that in specimens cold-reduced 0 and 5 percent and then aged. Intense precipitation has occurred along the primary

deformation bands, especially where they are intersected by secondary slipbands (figs. 14(a) and (b), same region at two magnifications). Here again the substructure revealed by the electron micrographs corroborates the light microstructures of aged L-605 which has received 30-percent prior cold-rolling (fig. 5(c)).

The increased homogeneity of precipitation just described would be expected to provide improved mechanical properties. In the studies of references 12 and 13, increased room-temperature ductility and strength did indeed result when material cold-rolled to larger reductions of the order of 30 percent was aged for 50 and 1000 hours (figs. 2 and 3). It is apparent that a more homogeneous precipitate distribution similar to that observed in the present study in the prior-cold-worked L-605 after aging 1 hour had persisted through the longer aging times of 50 to 1000 hours. This in turn had resulted in the improved mechanical properties, especially ductility, relative to the alloy aged without prior cold work.

A small amount of matrix recrystallization was observed in this specimen, confirming Yukawa and Sato's observations (ref. 11), and earlier X-ray diffraction observations (refs. 12 and 13). It will be recalled that a decrease in room-temperature tensile strength was attributed to this partial recrystallization (ref. 12). A recrystallized grain in the same specimen is shown in figure 14(c). In figure 14(d) (50-hr aging), there appears to be both a completely recrystallized and an indeterminate (or incompletely recrystallized) region. Recrystallization is indicated in figure 14(c) by the following features which were predominant above the line B-B: the low dislocation density, the nearly random distribution of precipitate, and the somewhat vague outlines of annealing twins. The same features are predominant in the upper third of figure 14(d). However, the interface between the two regions in figure 14(d) appears diffuse rather than sharply defined, as would be expected of an advancing recrystallization front. We may be observing here early stages of formation of recrystallization nuclei.

Precipitate particles within the recrystallized grains (see fig. 14(c)) appeared to be arranged somewhat preferentially along matrix crystallographic directions with respect to both distribution and shape, presumably corresponding to primary and secondary deformation bands; they were otherwise randomly distributed.

CONCLUDING REMARKS

Light microscopy and interpretation of the microstructures revealed thereby have heretofore provided qualitative understanding of the cold-working-aging treatment variables for L-605 and their effects on mechanical properties. The present study has extended this qualitative understanding to the substructural level through direct observations of thin foils in the electron microscope. A logical direction for future research on

this and similar alloys would entail utilizing the additional capabilities of direct transmission thin foil electron microscopy combined with other techniques to provide quantitative understanding of the phenomena involved. Thus, changes in location and morphology of the individual precipitating phases resulting from use of prior cold work may relate significantly to alterations in mechanical properties. Use of a series of aging temperatures and times to develop the full range of precipitates, in combination with use of electron microscopy and diffraction analysis to characterize fully each phase in situ, would provide this information. For example, X-ray diffraction data (ref. 12) have suggested that the relative amount of M_6C carbide precipitate is decreased by application of prior cold work. It is expected that electron microscopy and corresponding electron diffraction could check the validity of as well as explain this phenomenon and thus contribute to an appraisal of its significance.

The role of cold work in inducing the fcc to hcp transformation in this alloy and in cobalt-base superalloys generally has been inadequately defined. How, when, and to what extent this occurs, both during the cold deformation and during subsequent aging, may be important to service performance. Development of this information would require a well rounded program encompassing a number of cold-working and aging treatments and the full range of evaluating techniques used in the present study, including especially quantitative electron microscopy (imaging plus diffraction analysis).

Knowledge of the details of the partial-dislocation collapsing process during aging would certainly contribute to a total understanding of the thermomechanical processing details and their effects on mechanical properties in L-605 and other cobalt-base superalloys. A hot stage electron microscopy study in which specimens are observed continually during the aging process should provide much of the needed information. It is presently speculated on the basis of observations reported in the literature, and of those made in the present investigation that the aging process so depletes the matrix in one or more alloying elements that its stacking fault energy is increased to the point where energy considerations prevent significant dissociation of dislocations into partials. On the other hand, simple relaxation of residual stresses during the aging may be a major or even the dominant factor. A hazard in this type of study would be the possiblity that aging processes in the thin foils might not be representative of those in the bulk material, as a result of relaxation of restraints or increased surface-energy effects in the nearly two-dimensional electron microscope foils. This would, or course, have to be taken into account in any such evaluation.

SUMMARY OF RESULTS

The following observations were made during a thin-foil transmission electron microscopy study of the cobalt-base alloy L-605 (HS-25) in four conditions: mill-annealed; mill-annealed and cold-worked; mill-annealed and aged; and mill-annealed, cold-worked, and aged. Cold-work reductions up to 30 percent and aging times of 1 to 50 hours were used.

1. Application of moderately severe cold-working (rolling) between annealing and aging of L-605 sheet was shown to introduce many intragranular nucleation sites, mainly slipband intersections, at which precipitate particles formed during aging at 1600° F (871° C). Thus, in accordance with accepted age-hardening principles, precipitation within the grains increased relative to that in grain boundaries, as a result of the 30-percent cold-rolling prior to the 1-hour aging. These results were in complete agreement with previous light-microscopy observations concerning the effects of prior cold work on the structure of L-605.

2. There is a clearly implied cause and effect relation between this more homogenous precipitation and the improved room-temperature ductility and strength previously reported after cold-rolling and aging for much longer times (up to 1000 hr).

Some specific observations from the transmission electron microscopy studies are as follows:

3. Cold-working of the mill-annealed material greatly increased the density of extended dislocations and their associated stacking faults.

4. Slip produced by cold-working (rolling) was nonhomogeneous, being concentrated in deformation bands ("bundles of stacking faults") which probably include some thin regions of hexagonal-close-packed matrix, as well as the extended dislocations.

5. Within a given grain, as a result of small (5-percent) cold reductions the deformation bands corresponded predominantly to one slip system. With increased amounts of cold deformation (30-percent reduction), the primary deformation bands became sheared by the operation of secondary slip systems.

6. With aging at 1600° F (871° C), extended partial dislocations generally collapsed to total dislocations, eliminating most of the stacking faults. This occurred in specimens of both prior conditions (as annealed, and annealed and cold-worked).

7. With aging, most or all of the deformation bands appeared to change from bundles of stacking faults (usually bounded by pairs of partial dislocations) to tangles or arrays of total dislocations, which were preferred sites for precipitate nucleation. The intersections of secondary slipbands with the primary bands appeared to be especially favored sites for nucleation. The end result, which corroborated previously published observations, was a more uniform intragranular distribution of precipitate particles, as opposed to predominantly grain-boundary precipitate in unworked material.

8. Regions which appeared to be recrystallized were observed in a specimen which had been aged 50 hours at 1600° F (871° C) after 30-percent cold reduction. However, the expected well-defined interface between recrystallized and unrecrystallized regions was not observed. In a "recrystallized" region, precipitates appeared to have some tendency toward preferred arrangement of particles along two or more matrix crystallographic directions but were otherwise randomly distributed.

Lewis Research Center,
National Aeronautics and Space Administration,
Cleveland, Ohio, October 21, 1970,
129-03.

REFERENCES

1. Kotval, P. S.: The Microstructure of Superalloys. Metallography, vol. 1, Jan. 1969, pp. 251-285.

2. Lux, B.; and Bollmann, W.: Precipitation Hardening of Co-Base Alloys by Means of an Intermetallic Co-Mo Phase. Cobalt, no. 11, June 1961, pp. 4-20.

3. Lux, B.; and Bollmann, W.: On the Mechanism of Carbide Precipitation in Cobalt-Base, Heat-Resistant Alloys during Age-Hardening. Cobalt, no. 12, Sept. 1961, pp. 32-38.

4. Habraken, L.: Electron-Microscope Study of A Cobalt-Base Alloy. J. Inst. Metals, vol. 90, 1961-62, pp. 85-92.

5. Habraken, L.; and Coutsouradis, D.: Tentative Synthesis on the Role of Cobalt in High-Strength Alloys. Cobalt, no. 26, Mar. 1965, pp. 10-24.

6. Drapier, J. M.; de Brouwer, J. L.; and Coutsouradis, D.: Refractory Metals and Intermetallic Precipitates in Cobalt-Chromium Alloys. Cobalt, no. 27, June 1965, pp. 59-72.

7. Rogister, C.; Coutsouradis, D.; and Habraken, L.: Improvement of Heat-Resisting Cobalt-Base Alloys by Precipitation Hardening. Cobalt, no. 34, Mar. 1967, pp. 3-9.

8. Drapier, J. M.; and Coutsouradis, D.: Precipitation Hardening of Co-Cr-Ta Alloys. Cobalt, no. 39, June 1968, pp. 63-74.

9. Drapier, J. M.; Leroy, V.; Dupont, C.; Coutsouradis, D.; and Habraken, L.: Structural Stability of Mar-M 509, a Cobalt-Base Superalloy. Cobalt, no. 41, Dec. 1968, pp. 199-213.

10. Woulds, Michael J.; and Cass, Thomas R.: Recent Developments in MAR-M Alloy 509. Cobalt, no. 42, Mar. 1969, pp. 3-13.

11. Yukawa, N.; and Sato, K.: The Correlation Between Microstructure and Stress Rupture Properties of a Co-Cr-Ni-W (HS-25) Alloy. Trans. Japan Inst. Metals, vol. 9, 1968 (Supplement), pp. 680-686.

12. Sandrock, Gary D.; and Leonard, L.: Cold Reduction as a Means of Reducing Embrittlement of a Cobalt-Base Alloy (L-605). NASA TN D-3528, 1966.

13. Sandrock, G. D.; and Leonard L.: Effect of Cold Reduction on Precipitation and Embrittlement of a Cobalt-Base Alloy (L-605). Cobalt, no. 33, Dec. 1966, pp. 171-175.

14. Nejedlik, J. F.: The Embrittlement Characteristics of a Low-Silicon Modified Cobalt-Base Alloy (L-605) at 1200° and 1600° F. Rep. ER-6870, TRW, Inc., June 15, 1966.

15. Wlodek, S. T.: Embrittlement of a Co-Cr-W (L-605) Alloy. Trans. ASM, vol. 56, no. 3, Sept. 1963, pp. 287-303.

16. Anon.: Alloy Sheet, Corrosion and Heat Resistant Cobalt Base, 20Cr-10Ni-15W. Aerospace Material Specification No. AMS 5537B, June 30, 1962.

17. Sandrock, Gary D.; Ashbrook, Richard L.; and Freche, John C.: Effect of Variations in Silicon and Iron Content on Embrittlement of a Cobalt-Base Alloy (L-605). NASA TN D-2989, 1965.

18. Sandrock, Gary D.; Ashbrook, Richard L.; and Freche, John C.: Effect of Silicon and Iron Content on Embrittlement of a Cobalt-Base Alloy (L-605). Cobalt, no. 28, Sept. 1965, pp. 111-114.

19. Hirsch, P. B.; Howie, A.; Nicholson, R. B.; Pashley, D. W.; and Whelan, M. J.: Electron Microscopy of Thin Crystals. Butterworths Co., 1965, p. 58.

20. Kotval, P. S.: Carbide Precipitation on Imperfections in Superalloy Matrices. Trans. AIME, vol. 242, no. 8, Aug. 1968, pp. 1651-1656.

TABLE I. - SUMMARY OF PRECIPITATED PHASES FOUND IN L-605

[Data from ref. 11.]

Phase	Structure	Lattice parameters, Å(10^{-10}m)
M_7C_3	Hexagonal (trigonal)	a = 13.98 c = 4.52 c/a = .33
$M_{23}C_6$	Face-centered cubic	a = 10.55 ~ 10.68
M_6C	Face-centered cubic	a = 10.99 ~ 11.22
α-Co_3W	$L1_2$-ordered face-centered cubic	a = 3.57
β-Co_3W	$D0_{19}$-ordered hexagonal	a = 5.11 c = 4.10 c/a = .80
Laves-Co_2W	C14-hexagonal	a = 4.73 c = 7.70 c/a = 1.63
μ-Co_7W_6	$D8_5$-hexagonal (rhombohedral)	a = 4.73 c = 25.5 c/a = 5.39

TABLE II. - COMPOSITION OF L-605 (HS-25)

[Data from ref. 12.]

Element	Aerospace Materials Specification,[a] wt %	Composition of heat investigated, wt % (b)
Chromium	19 to 21	20.07
Tungsten	14 to 16	14.62
Nickel	9 to 11	10.06
Iron	[c]3	1.67
Manganese	1 to 2	1.52
Silicon	[c]1	.63
Carbon	0.05 to 0.15	.08
Phosphorous	[c]0.04	.012
Sulfur	[c]0.03	.011
Cobalt	Balance	Balance

[a]AMS 5537B (ref. 16).
[b]As determined by supplier.
[c]Maximum.

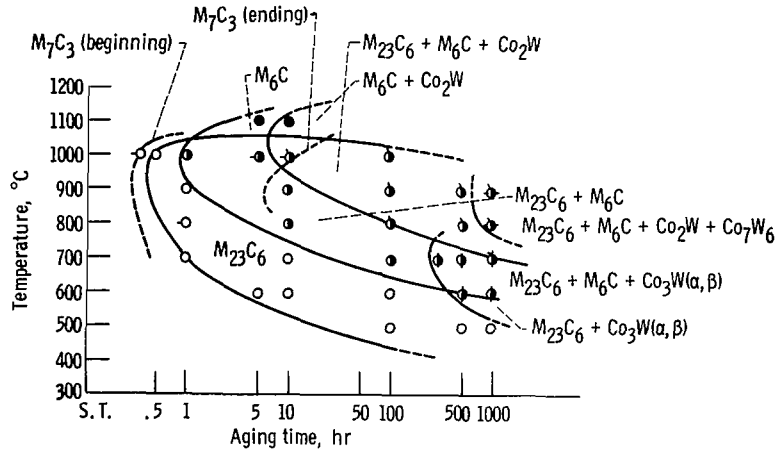

Figure 1. - Time-temperature-transformation diagram of HS-25 alloy showing its precipitation behavior (ref. 11). Alloy composition in weight percent: 0.05 carbon, 1.56 manganese, 0.85 silicon, 20.06 chromium, 9.81 nickel, 14.88 tungsten, 0.23 iron, balance cobalt. Solution treated at 1230° C for 1/2 hour, water quenched.

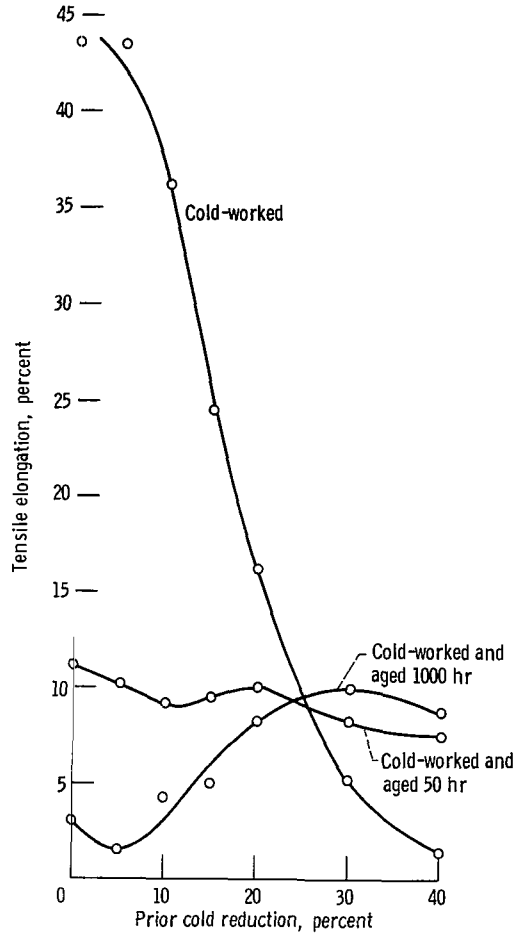

Figure 2. - Effect of prior cold reduction on room-temperature ductility of mill-annealed L-605 before aging and after aging 50 and 1000 hours at 1600° F (871° C) (ref. 12).

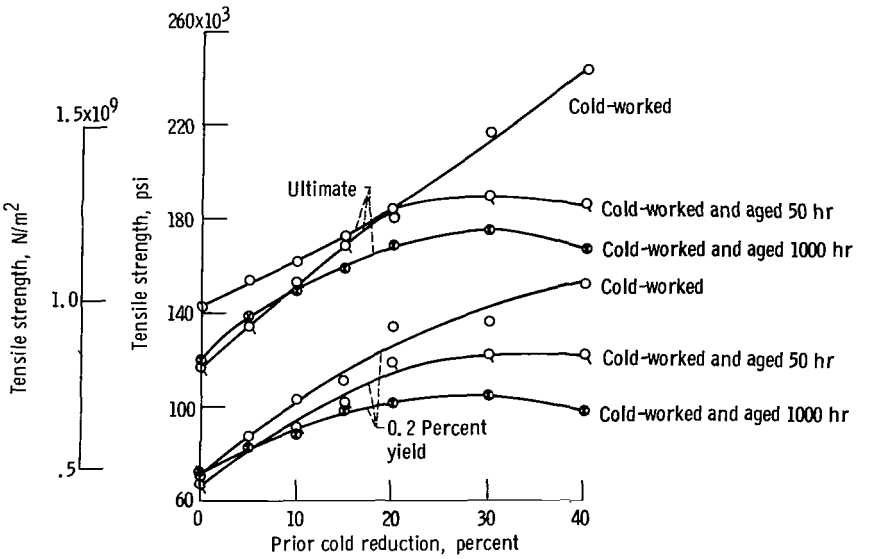

Figure 3. - Effect of prior cold reduction on room-temperature tensile strength of annealed L-605 before aging and after aging 50 and 1000 hours at 1600° F (871° C) (ref. 12).

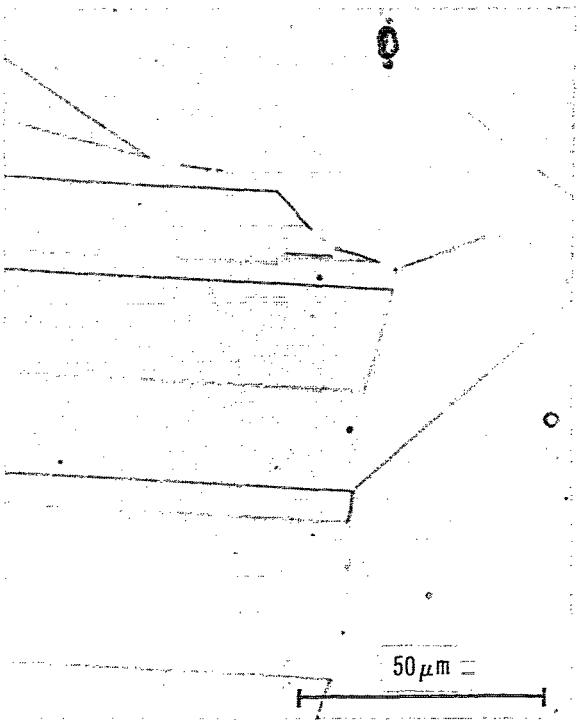

(a) 0-Percent cold-rolled.

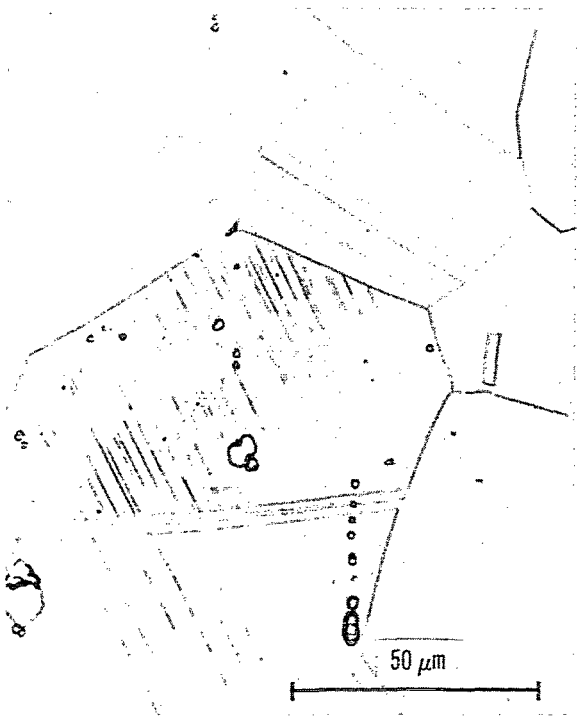

(b) 5-Percent cold-rolled.

(c) 30-Percent cold-rolled.

Figure 4. - Effect of cold reduction on microstructure of mill-annealed L-605. Etchant, hydrochloric acid and hydrogen peroxide (ref. 12).

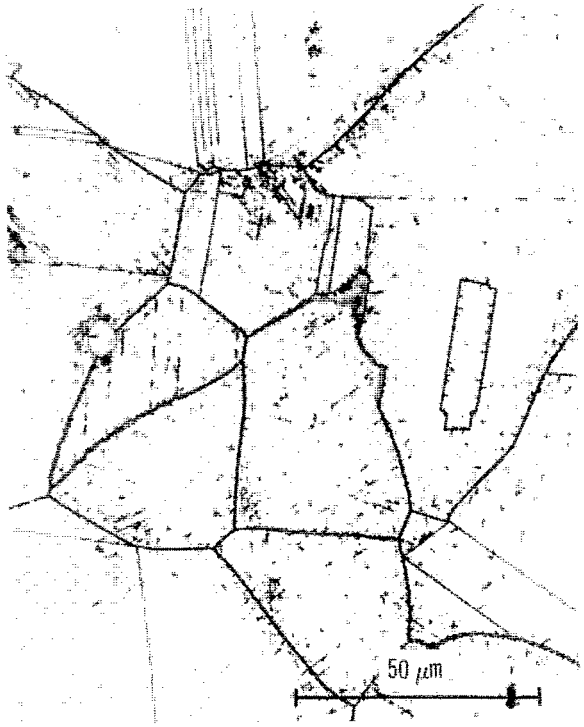

(a) 0-Percent cold-rolled.

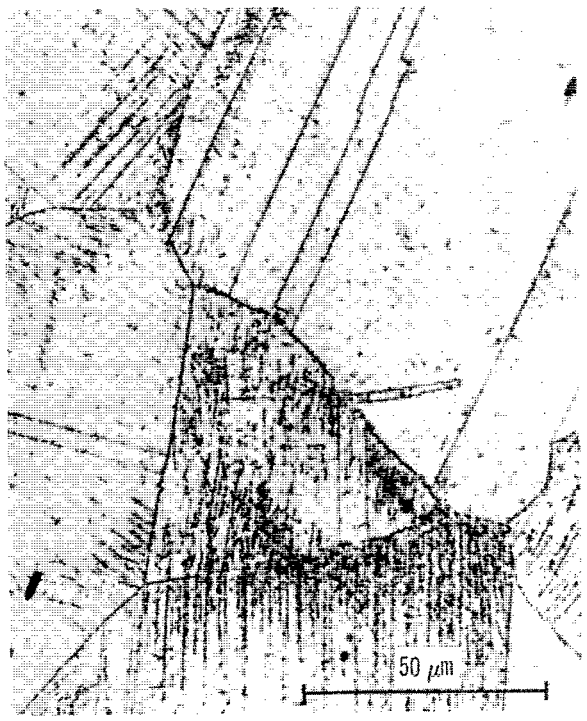

(b) 5-Percent cold-rolled.

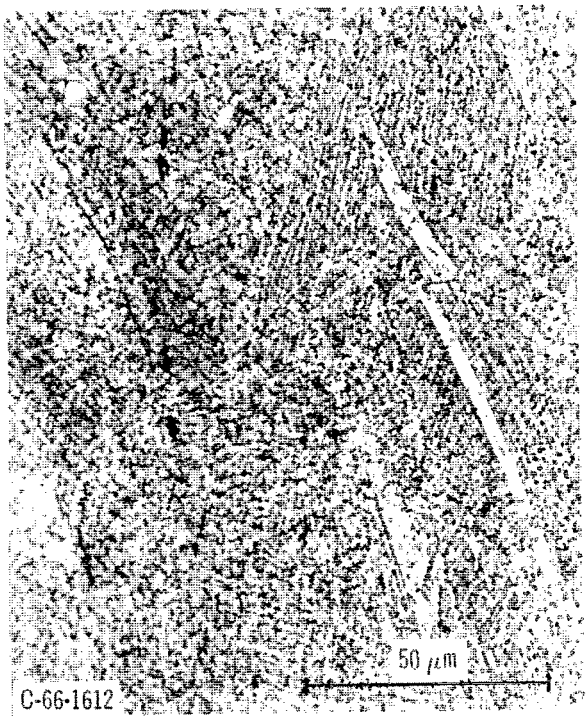

(c) 30-Percent cold-rolled.

Figure 5. - Effect of prior cold reduction on microstructure of L-605 after aging 50 hours at 1600° F (871° C). Etchant, boric acid and sulfuric acid (ref. 12).

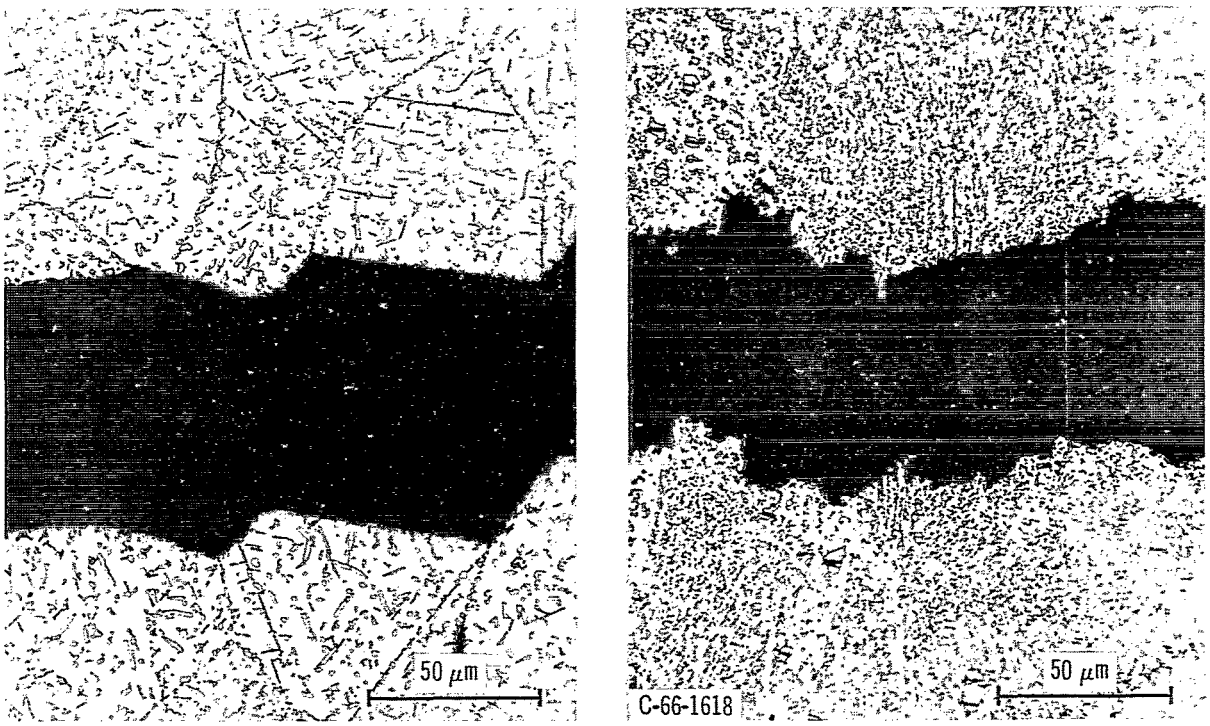

(a) 0-Percent cold-rolled.

(b) 30-Percent cold-rolled.

Figure 6. - Effect of prior cold reduction on tensile fracture of L-605 aged 1000 hours at 1600° F(871° C). Etchant, boric acid and sulfuric acid (ref. 12).

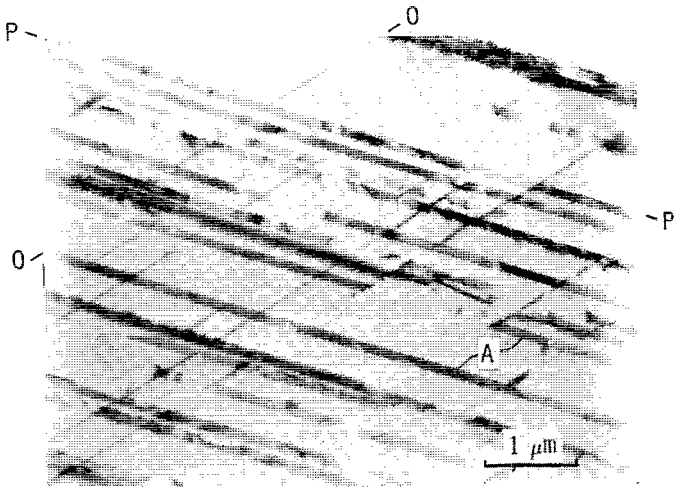

(a) Region of relatively long semicontinuous stacking faults.

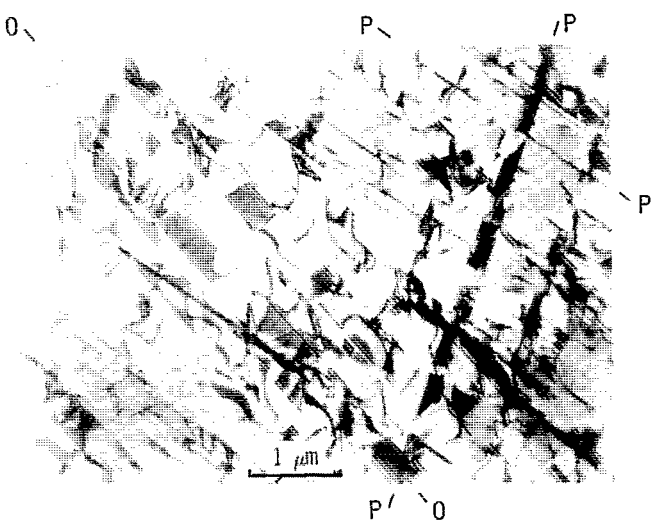

(b) Region characterized by moderately extended dislocations.

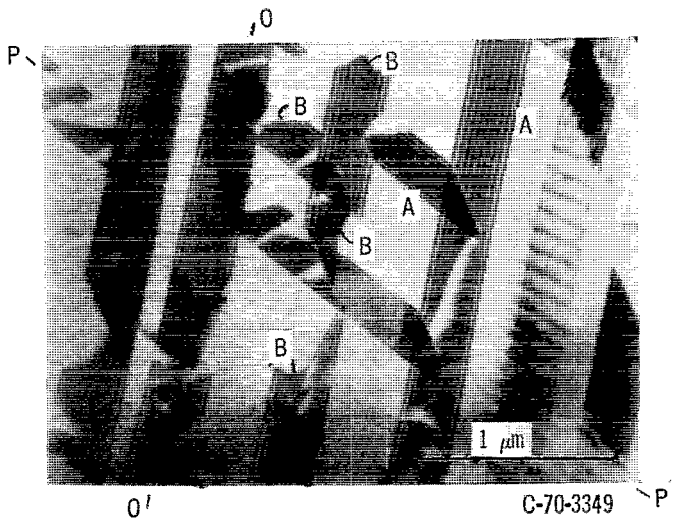

(c) Higher magnification of foil region showing distinctly resolved stacking-fault fringes (or ribbon contrast).

Figure 7. - Thin foil substructures of L-605 as mill-annealed, showing a relatively low density of extended dislocations on {111} planes (0-0, P-P, R-R) with ribbon-contrast stacking faults, (some indicated by letter A), each bounded by a pair of partial dislocations (some indicated by letter B).

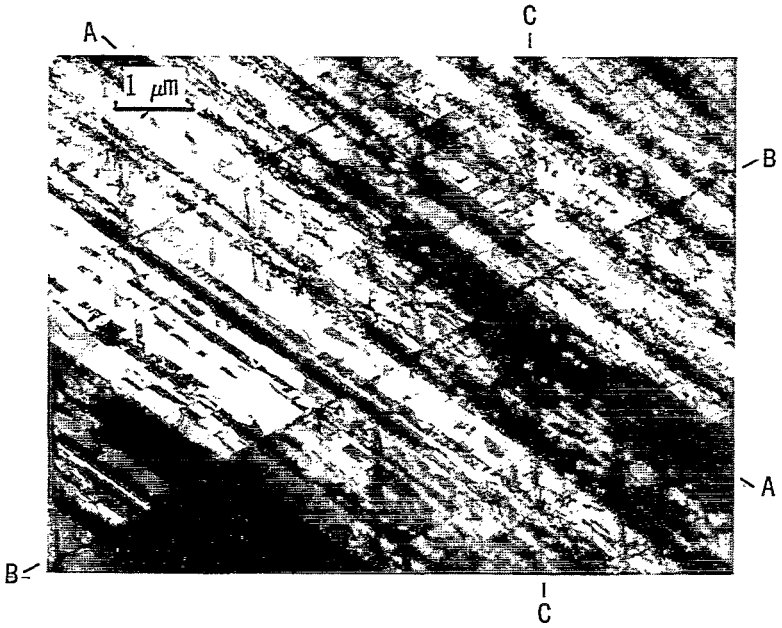

(a) Predominant slip on one system (direction A-A), with evidence of lesser activity on two other slip systems (directions B-B and C-C).

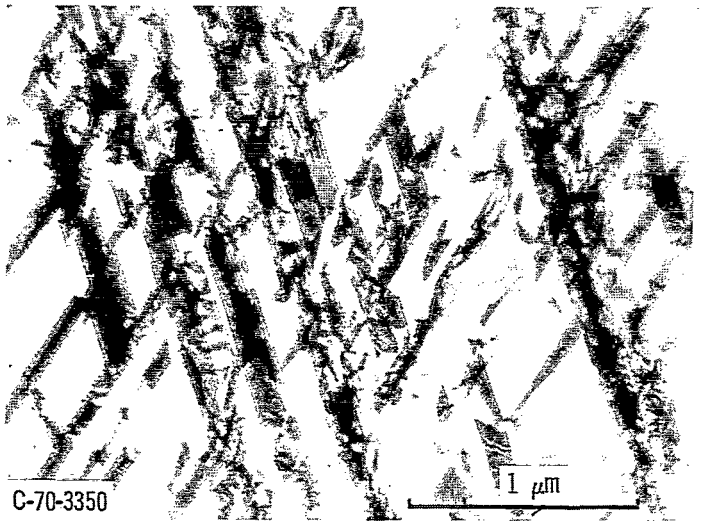

(b) At higher maginfication, randomly distributed, slightly extended dislocations apparent on predominant slip systems. Different area and foil orientation from figure 8(a).

Figure 8. - Substructures in thin foil of L-605 mill-annealed and cold-rolled 5 percent. Density of extended dislocations is increased relative to figure 7, and distribution of slip is not homogeneous, as shown by clustering of slip dislocations into "bundles" (slipbands, e.g., A-A; compare figs. 8(a) and 7(a)).

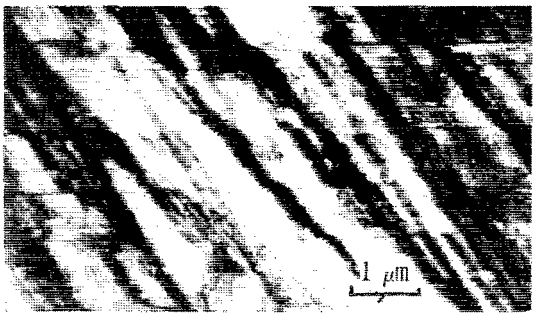

(a) Substructure.

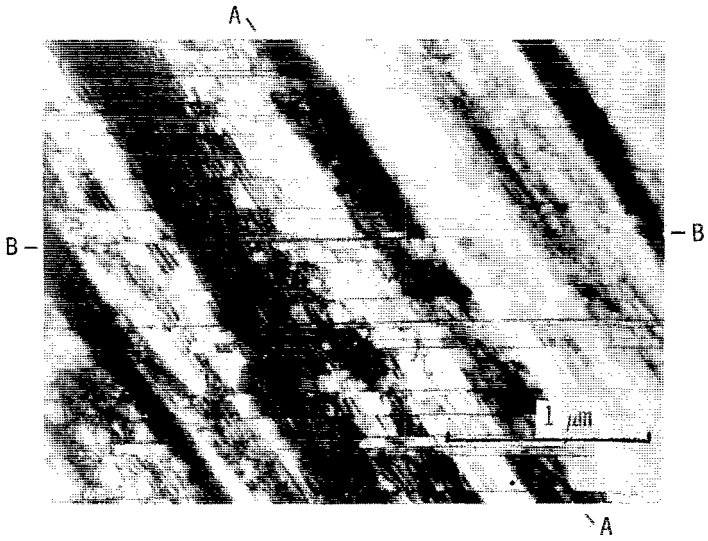

(b) Area similar to that shown in (a) at higher magnification.

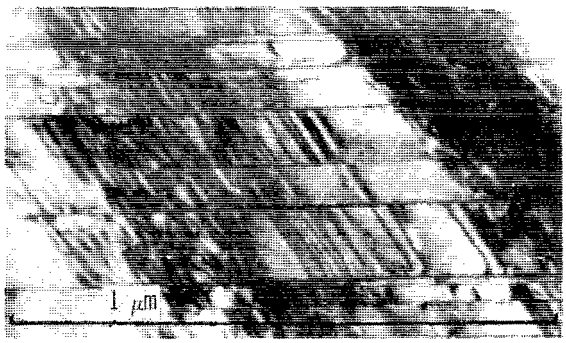

(c) Area similar to those shown in (a) and (b) at higher magnification.

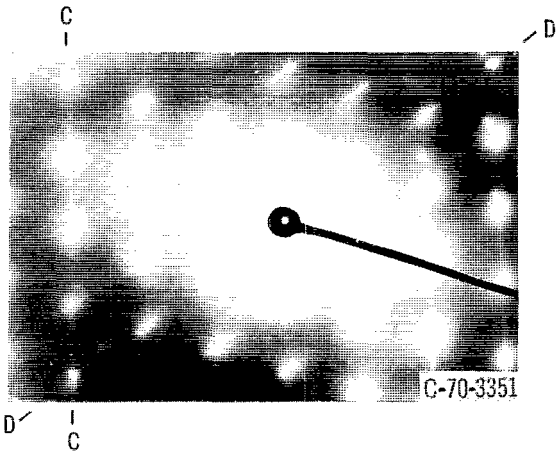

(d) Selected-area diffraction pattern corresponding to (b). Note nearly continuous streaks C-C normal to "edge-on" slipbands on (111) planes of (b) (e.g., B-B) and shorter, less-regular streaks (D-D) normal to primary slipbands of (b) (e.g., A-A).

Figure 9. - Substructure of mill-annealed and 30-percent-cold-rolled L-605, with corresponding diffraction pattern. Note increased intensity and density of extended-dislocation slipbands on primary (111) slip planes (direction A-A in (b)), parallel to $[1\bar{1}0]$ direction of micrograph. Also, note slipbands on secondary $(\bar{1}\bar{1}1)$ planes (direction B-B in (b)), parallel to $[\bar{1}12]$ direction of micrograph. Discontinuities in primary slipbands introduced by subsequent activity on secondary slip system are apparent. Plane of foil is nearly (110).

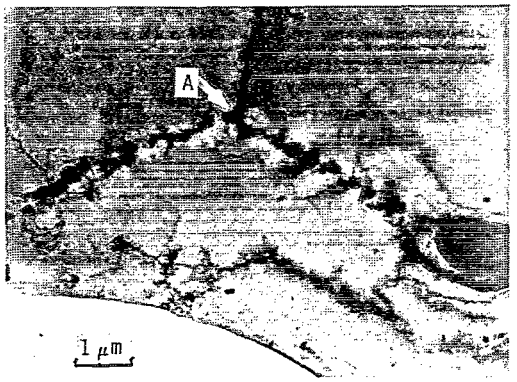

(a) Coarse precipitate particles in grain boundary near triple point (A).

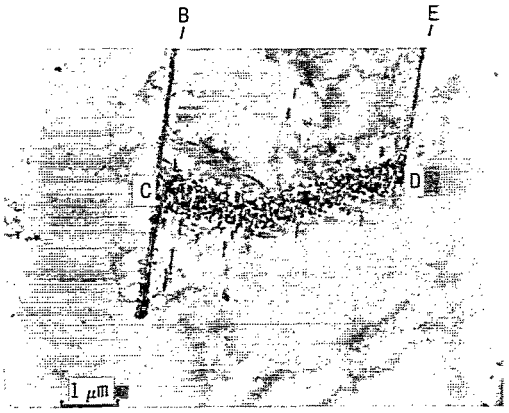

(b) Somewhat finer particles around end of annealing twin (B-C-D-E).

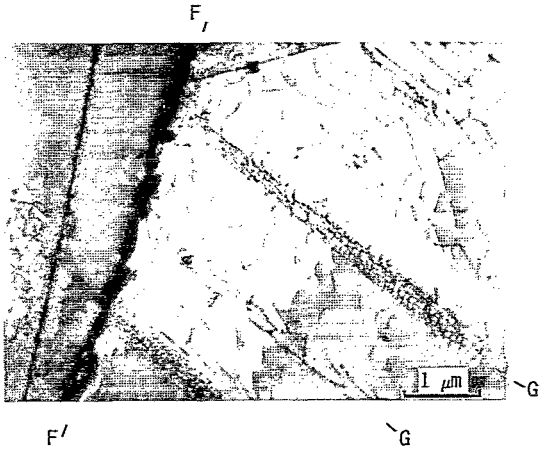

(c) Precipitation along grain boundary (F-F). Note absence of stacking faults. Arrays and networks of dislocations (G) are evident which probably are related to stacking faults of unaged L-605 (see figure 7).

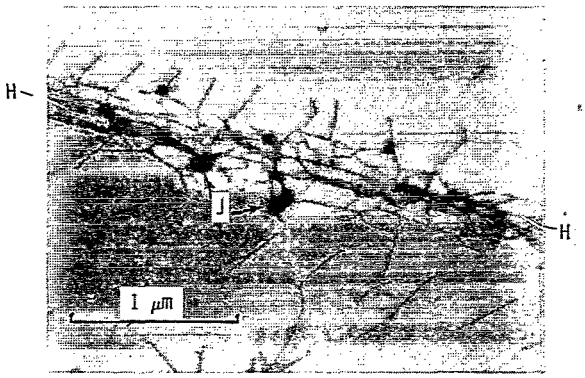

(d) Detail of dislocation network (H-H), showing occasional particles (J) apparently precipitated on dislocations.

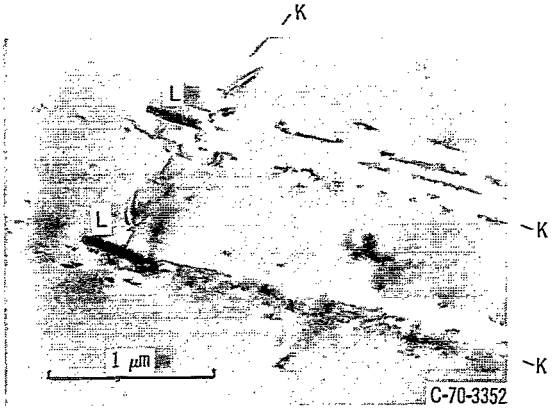

(e) Features interpreted to be dislocations in slipband arrays (K) plus a few precipitate particles (L) which have nucleated on dislocations.

Figure 10. - Effects of aging at 1600° F (871° C) for 1 hour without prior cold work on substructure in mill-annealed L-605. Note predominance at grain and twin boundaries of precipitate nucleation and essentially complete absence of stacking faults (i.e., "collapse" of extended dislocations has occurred).

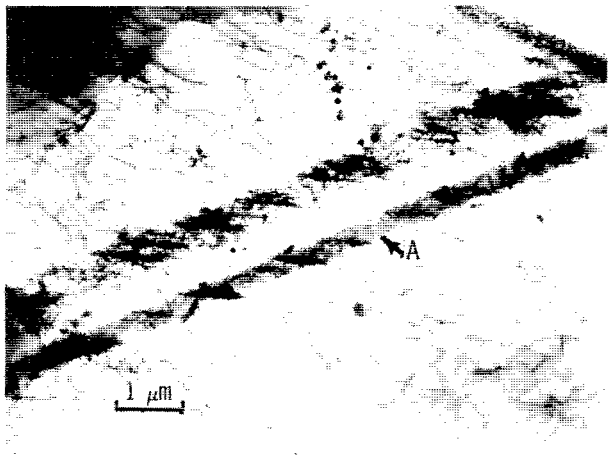

(a) Region of foil at moderate magnification.

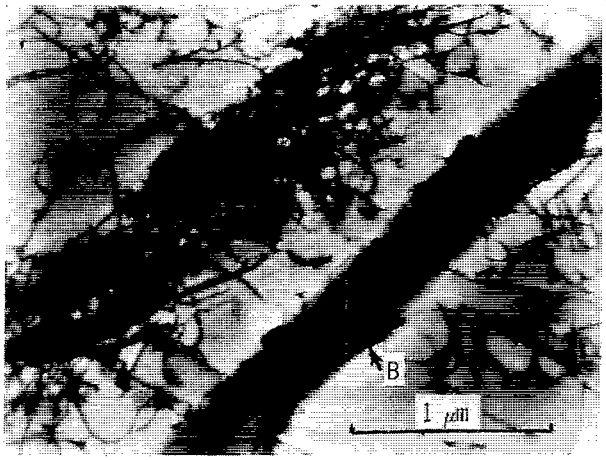

(b) Same region as in (a) at higher magnification, showing evidence of preferred nucleation on dislocations in slipbands (e.g., B).

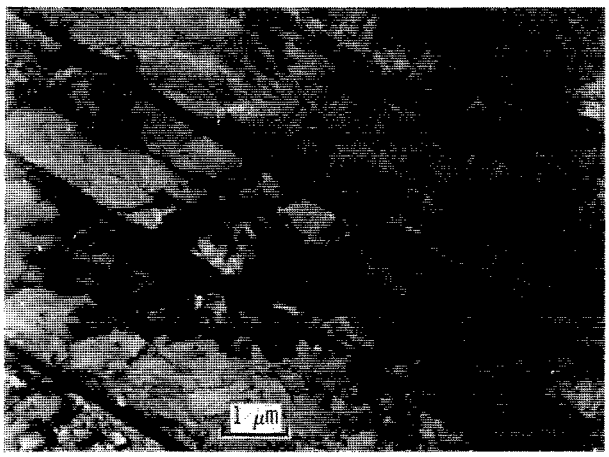

(c) Another region of same foil as in (a) and (b) illustrating preferred precipitate nucleation at slipband intersections.

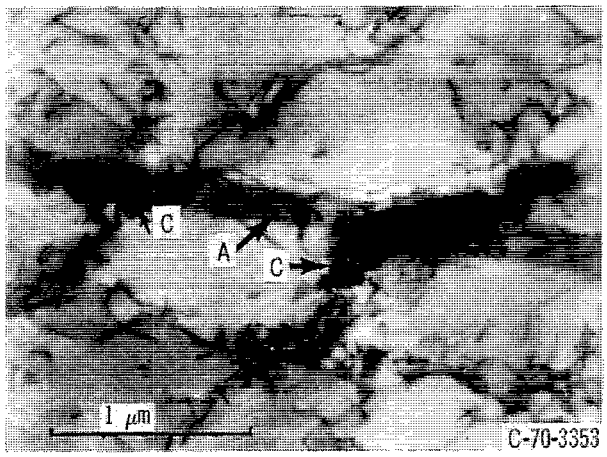

(d) Same region as in (c) at higher magnification. Note preferred precipitate nucleation at slipband intersections (e.g., C), between stacking fault (A) and dislocation tangle arrays (D-D).

Figure 11. - Effects of cold-rolling 5 percent and aging at 1600° F (871° C) for 1 hour, on substructure in mill-annealed L-605. Note evidence of a few extended dislocations (A) and of preferred precipitate nucleation at slipband intersections.

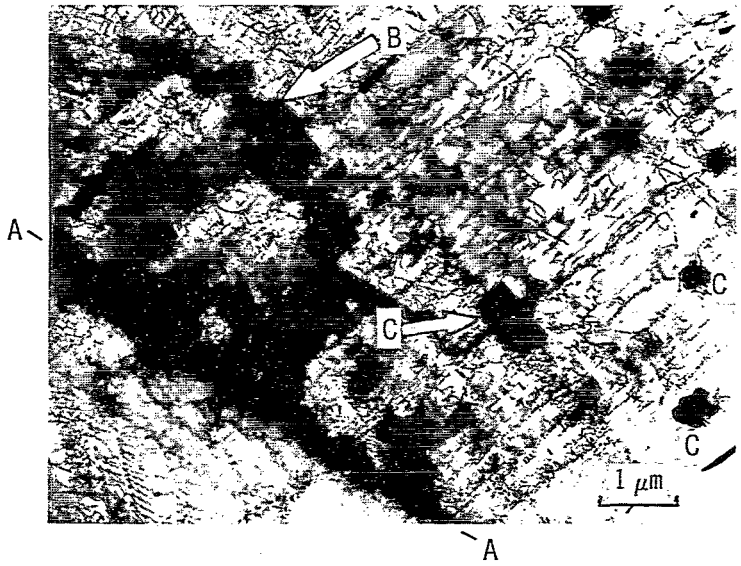

(a) Relatively coarse precipitates predominantly in grain boundary (A-A), plus some precipitates (B and C) within a grain.

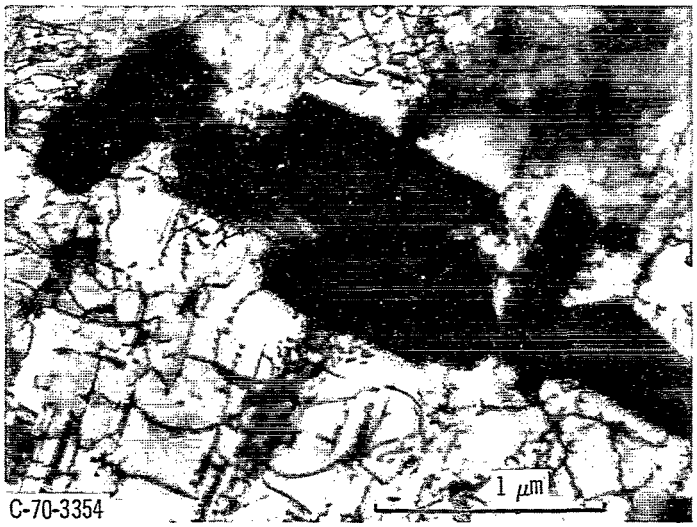

(b) Precipitate cluster (B) from upper left of micrograph, at higher magnification.

Figure 12. - Precipitation occurence and morphology in mill-annealed L-605 which has been cold-rolled 5 percent and aged at 1600° F (871° C) for 7 hours.

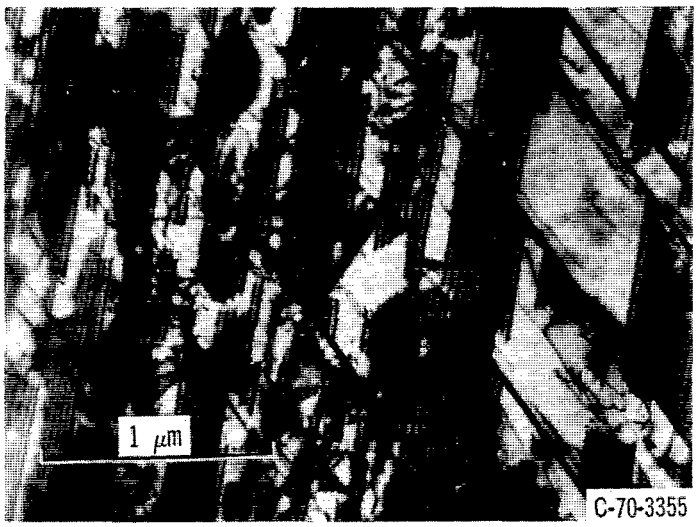

Figure 13. - Region of same specimen as shown in figure 12, which reveals unusual concentration of extended dislocations and associated stacking faults for aged specimen. This condition is possibly an "artifact" resulting from accidental mechanical deformation during specimen preparation or handling.

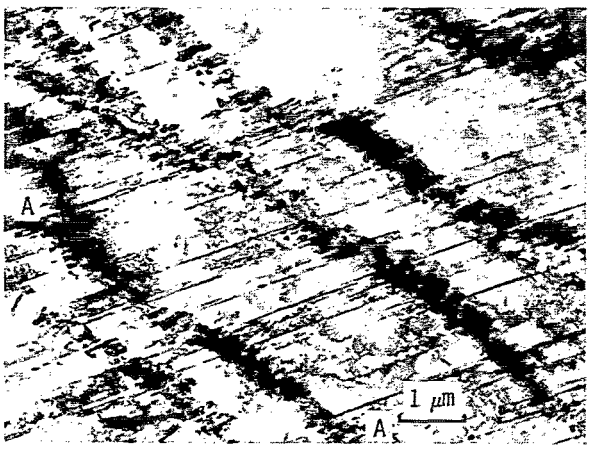

(a) Typical intense precipitation along slipbands (e.g., A-A), in foil aged for 1 hour.

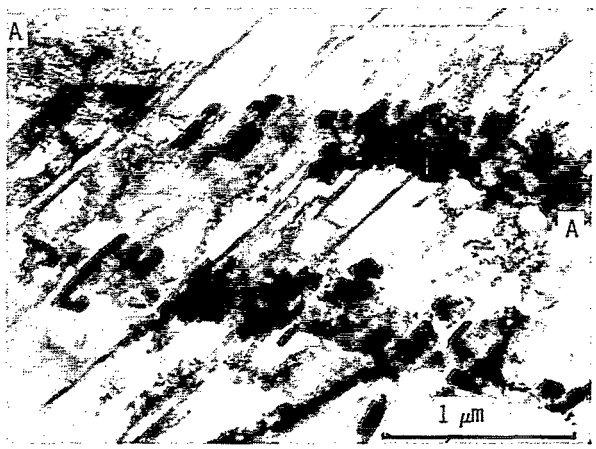

(b) Same region of foil as in (a) at higher magnification.

(c) Recrystallized region in same specimen as in (a) and (b), showing semirandom precipitation distribution. Note general reduced density of dislocations, except at lower right below line B-B. Also, relatively random distribution of precipitate, and presence of parallel-sided annealing twins, as indistinctly outlined parallel to C-C.

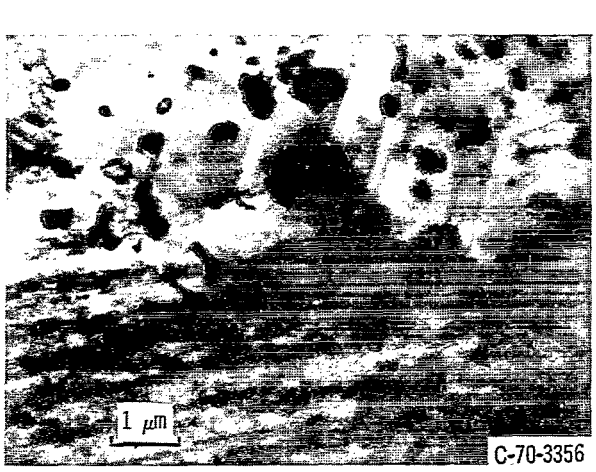

(d) Recrystallized region in similar specimen (aged for 50 hr), showing characteristics of (a) and (b), as well as of (c).

Figure 14. - Effects of cold-rolling 30 percent and aging at 1600° F (871° C) on substructure of mill-annealed L-605.

"The aeronautical and space activities of the United States shall be conducted so as to contribute . . . to the expansion of human knowledge of phenomena in the atmosphere and space. The Administration shall provide for the widest practicable and appropriate dissemination of information concerning its activities and the results thereof."

—NATIONAL AERONAUTICS AND SPACE ACT OF 1958

NASA SCIENTIFIC AND TECHNICAL PUBLICATIONS

TECHNICAL REPORTS: Scientific and technical information considered important, complete, and a lasting contribution to existing knowledge.

TECHNICAL NOTES: Information less broad in scope but nevertheless of importance as a contribution to existing knowledge.

TECHNICAL MEMORANDUMS: Information receiving limited distribution because of preliminary data, security classification, or other reasons.

CONTRACTOR REPORTS: Scientific and technical information generated under a NASA contract or grant and considered an important contribution to existing knowledge.

TECHNICAL TRANSLATIONS: Information published in a foreign language considered to merit NASA distribution in English.

SPECIAL PUBLICATIONS: Information derived from or of value to NASA activities. Publications include conference proceedings, monographs, data compilations, handbooks, sourcebooks, and special bibliographies.

TECHNOLOGY UTILIZATION PUBLICATIONS: Information on technology used by NASA that may be of particular interest in commercial and other non-aerospace applications. Publications include Tech Briefs, Technology Utilization Reports and Technology Surveys.

Details on the availability of these publications may be obtained from:

SCIENTIFIC AND TECHNICAL INFORMATION OFFICE

NATIONAL AERONAUTICS AND SPACE ADMINISTRATION

Washington, D.C. 20546